COLLISION THEORY APPLICATION TO INVESTIGATE RAPPING HAMMER FORCE AND ELECTRODE FRAME LIFESPAN IN DUST FILTERS

Nguyen Anh Tung[1], Hoang Van Got[2*], Nguyen Tien Sy[3], Nguyen Duc Toan[4]

Article History: **Received:** 28.03.2023 **Revised:** 29.04.2023 **Accepted:** 06.05.2023

Abstract

The cyclic impact of rapping hammers against the collecting electrode frame of horizontal electrostatic precipitators creates a collision between the hammer and the anvil beam end of the collecting electrode frame. This collision generates periodic vibrations that dislodge dust from the surface of the collecting electrode plates and discharge electrodes, facilitating dust removal. This article presents a scientific explanation of stress wave propagation in the collecting electrode plates, which accelerates dust removal while causing fatigue damage to important components such as the collecting plates, discharge electrode frames, and rapping hammers. To address this scientific challenge, the collision theory of two rigid bodies has been applied, and experimental verification has been conducted on a filter chamber model to determine the acceleration of stress wave propagation and the durability of the collecting electrode plates. This study offers insights that can inform the design and optimization of dust filter chambers, leading to enhanced efficiency and effectiveness in industrial dust removal processes.

Keywords: Rapping hammers, Horizontal electrostatic precipitators, Dust removal, Stress wave propagation, Filter chamber model

[1,2*]Associate Professor, National Research Institute of Mechanical Engineering. Address: No. 4, Pham Van Dong streets, Cau Giay, Ha Noi
[3]Hanoi University of Industry, No. 298 Cau Dien Street, Bac Tu Liem District, Hanoi, Vietnam
[4]School of Mechanical Engineering, Hanoi University of Science and Technology, 1st Dai Co Viet Road, Hai Ba Trung District, Hanoi 100000, Vietnam

Email: [2*]gotnarime@yahoo.com.vn

DOI: 10.31838/ecb/2023.12.1.273

1. Introduction

The treatment and filtration of emission gases from power plants, cement, and construction material plants is an urgent issue worldwide. In Vietnam, there are more than 100 generating units in thermal power plants, and hundreds of electrostatic precipitators are used in these plants. The filter chamber, which comprises plate-type dust collecting electrodes serving as the cathode and spiked rod-type discharge electrodes that ionize the dust particles, is the most vital component. The exhaust gas from coal-fired boilers entering the filter chamber has a high dust content of about 250-300 mg/Nm3, and the output exhaust gas must be reduced to 50-100 mg/Nm3, depending on the surrounding air environment requirements [1-7].

Although electrostatic precipitators in Vietnam have been fully imported from foreign suppliers for several decades, the National Research Institute of Mechanical Engineering has recently designed and supplied equipment for several domestic projects, such as Vung Ang 1 TPP, Thai Binh 2 TPP, and Nghi Son 2 TPP. However, the scientific determination of the collecting electrode's durability concerning the cyclic impact force of the rapping hammer remains a crucial topic that requires further investigation.

The collecting and discharge electrodes are mechanically connected into a unified structure but insulated from each other. The electrodes' durability meets the design requirements, and their efficiency is high. However, if one of the electrodes is damaged, the generating unit must stop working. With hundreds of electrostatic precipitators operating in Vietnam today, this can cause significant losses [3]. Therefore, domestic research and design focused on determining the appropriate durability of the collecting electrode plates to serve the localization purpose is an urgent issue in Vietnam today.

2. Methodology and Research

This section presents the theoretical framework and methodology used in this study to analyze the radial collision of two perfectly rigid bodies. The theory of radial collisions is based on the collision between two bodies in translational motion that collide at point I. The velocity of the centers of mass before the collision is represented by $\overrightarrow{v_1}$ and $\overrightarrow{v_2}$ respectively. The line connecting the two centers of mass of two bodies C1C2 is called the radial line, and the common normal of two contact surfaces of two bodies at line n_1In_2 is called the collision line (Figure 1). The collision impulse during the deformation and recovery phases of the elastic collision is represented by $\overrightarrow{S_1}$ and $\overrightarrow{S_2}$ respectively.

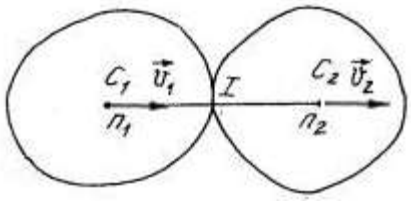

Figure 1. Diagram of radial collision of two solids

The collision phases start when two bodies come into contact with each other with different velocities and end when they reach the same velocity $\vec{u}$ during the deformation phase. The collision impulse during this period is $\overrightarrow{S_1}$. During the recovery phase, the collision starts when two bodies reach the same velocity (u ⃗) and end when the two bodies separate from each other with velocities $\overrightarrow{u_1}$ and $\overrightarrow{u_2}$. The collision impulse during this period is $\overrightarrow{S_2}$. The directions of impulses $\overrightarrow{S_1}$ and $\overrightarrow{S_2}$ are along the collision path C_1C_2, and friction at the contact point I is ignored. The formulae for collision during the deformation and recovery phases are given by equations (1) to (4). Equation (5) represents the third hypothesis about collisions, stating that the recovery factor is equal to the ratio of the impulse during the recovery phase to the impulse during the deformation phase.

$$m_1u - m_1v_1 = -S_1 \quad (1)$$

$$m_2u - m_2v_2 = S_1 \quad (2)$$
$$m_1u_1 - m_1u = -S_2 \quad (3)$$
$$m_2u_2 - m_2u = S_2 \quad (4)$$
$$S_2 = kS_1 \quad (5)$$

A radial collision occurs when the collision path n1In2 coincides with the radial line C1C2, and the velocities $\overrightarrow{v_1}$ and $\overrightarrow{v_2}$ are along the collision path and radial path. The velocity of the centers of mass of the two bodies after the collision is represented by $\overrightarrow{u_1}$ and $\overrightarrow{u_2}$, the momentum of the collision forces at each stage of the collision and the amount of kinetic energy lost in the collision. The recovery factor is represented by k. Equations (6) to (11) describe the momentum and recovery factor of the collision. Equation (6) represents the velocity of the centers of mass of the two bodies after the collision, while equation (7) represents the impulse during the deformation phase. Equation (8) represents the impulse during the recovery phase, and equation (9) and (10) represent the velocities of the two bodies after the collision. Equation (11) represents the recovery factor in terms of the relative velocities of the second body with respect to the first after and before the collision.

$$u = \frac{m_1v_1 + m_2v_2}{m_1 + m_2} \quad (6)$$
$$S_1 = \frac{m_1m_2}{m_1 + m_2}(v_1 - v_2) \quad (7)$$
$$S_2 = \mathrm{k}S_1 = k\frac{m_1m_2}{m_1 + m_2}(v_1 - v_2) \quad (8)$$
$$u_1 = v_1 - (1 + k)\frac{m_2}{m_1 + m_2}(v_1 - v_2) \quad (9)$$
$$u_2 = v_2 - (1 + k)\frac{m_1}{m_1 + m_2}(v_2 - v_1) \quad (10)$$
$$k = -\frac{u_2 - u_1}{v_2 - v_1} = -\frac{u_r}{v_r} \quad (11)$$

where v_r ang u_r are the relative velocities of the second body with respect to the first after and before the collisionThis study also uses the theory of stress wave propagation in thin metal sheets under impact force to analyze the collision of two perfectly rigid bodies. Moreover, the study determines the dust removal acceleration by experimental method. The methodology used in this study includes theoretical analysis, numerical simulation, and experimental validation. The methodology and research presented in this section provide a theoretical and practical framework for analyzing the radial collision of two perfectly rigid bodies. The equations derived in this section are essential for understanding the dynamics of the collision and for developing practical applications such as dust removal acceleration. The theoretical analysis, numerical simulation, and experimental validation provide a comprehensive approach for analyzing complex systems and phenomena.Phương pháp luận và nghiên cứu

Experiment for Determination of Dust Removal Acceleration of Stress Wave Propagation in ESP Collecting Electrode Plate

Development of the Formula for Calculating the Collision Between the Hammer and the Electrode Frame-Girder System

The experiment aimed to determine the acceleration of dust removal through stress wave propagation in an electrostatic precipitator (ESP) collecting electrode plate. To achieve this, a collision model was developed to simulate the impact of a hammer on the lower girder of the collecting electrode frame (Fig. 2). The model considers various factors, such as the weight of the hammer (m_1), mass of the collecting and discharge electrode set (m_2), height of the hammer for potential energy (H), angle of the hammer relative to the initial position (φ), and point of collision (c).

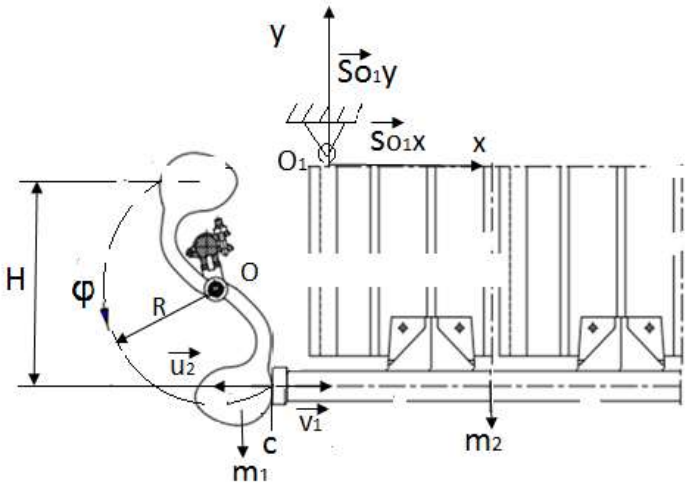

Figure 2. The collision model of the hammer rapping on the lower girder of the collecting electrode frame

To form the calculation formula, the impact of the hammer on the lower frame beam of the collecting electrode was modeled (Fig. 3). The potential energy values of the dust rapping system were determined from the diagram as T= ½ m1. R^2. φ^2 and π = mga cos φ. The Lagrange II's equation was then used to substitute these values and form the differential equation:

$$\frac{d}{dt}\left(\frac{\partial T}{\partial \dot{\varphi}}\right) - \frac{\partial T}{\partial \varphi} = \frac{\partial \pi}{\partial \varphi} \quad (12)$$

$$\ddot{\varphi} + g/Rsin\varphi = 0 \quad (13)$$

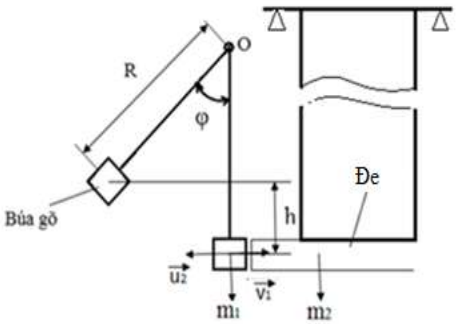

Figure 3. The collision model between the hammer and the lower frame beam of the collecting electrode

The speed of the hammer before impact (φ= π) was determined using the law of conservation of mechanical energy, which states that T + π = T^0 + π^0 = const. At the initial time (φ=0), T^0 = 0 , π^0 = 0 (φ = 0). Thus, T = - π at all times, where T is the kinetic energy of the hammer and π is its potential energy. The formula for the hammer's velocity before impact was then determined to be $v_1 = \sqrt{4.g.R}$.

The collision process was divided into two phases: the deformation phase and the recovery phase, with collision impulses S_1 and S_2, respectively. The law of momentum was applied to each stage. In the deformation phase, the collision impulses were calculated using the formulae:

$$\overrightarrow{S_1} = \int_0^r \overrightarrow{N_1 dt} \;\; ; \overrightarrow{S_2} = \int_0^r \overrightarrow{N_2 dt} \quad (14)$$

Where N_1 and N_2 are the normal forces during the deformation and recovery phases, respectively. In the deformation phase, the hammer and beam had the same speed (v). The collision impulses were then determined using the following equations:

Hammer: $m_1.v - m_1.v_1 = -S_1$

Beam: $m_2.v - m_2.v_2 = -S_2$ (15)

In the recovery phase, the hammer's velocity after collision (v_1') and the beam's velocity after collision (v_2') were calculated using the formulae:

Hammer: $m_1.v_1' - m_1.v = -S_2$ (16)

Beam: $m_2.v_2' - m_2.v = -S_2$ (17)

The recovery factor (k) was introduced, and the collision impulses were related as S_2= k.S_1. Finally, the hammer's velocity before impact (v_1) was substituted into the above equations to derive the following formulae:

$$\begin{cases} S_1 = \frac{m_1 m_2}{m_1+m_2}.v_1 = \frac{m_1 m_2}{m_1+m_2}.\sqrt{4gR} \\ S_2 = k.S_1 \end{cases} \quad (18)$$

$$\begin{cases} v_1' = v_1 - (1+k)\frac{m_2}{m_1+m_2}.v_1 \\ v_2' = v_2 + (1+k)\frac{m_2}{m_1+m_2}.v_1 \end{cases} \quad (19)$$

Schematic of experimental procedure for measuring stress wave acceleration in the collecting plate [3,6,7]

Stress wave propagating in the collecting electrode plate

The collecting electrode plate is made of rimming steel CTO, a special-purpose steel with a very low carbon content, and has a thickness of 1.2 mm. The plate has a total surface area of 15.500 x 5.760 m after assembly, which is much larger than its thickness, making it a thin, flat plate that facilitates the calculation of stress wave propagation conditions and collecting plate strength conditions using the method of mechanical reflection [1,5,7]. In practice, a hammer weighing between 5-10 kg is commonly used to rap on the collecting/discharge frame, which produces a small impact force. The force (F) applied by the hammer to the collecting electrode plate beam is calculated using the formula F = mg, where m is the mass of the hammer and g is the gravitational acceleration. Since the mass of the collecting electrode plate set and discharge electrode set is approximately 1000 kg, the ratio between the two masses is approximately 0.01. When the impact force is applied to the collecting electrode plate beam, a stress wave is created, which propagates through the collecting electrode plate, resulting in a propagating acceleration (a_i). Once the acceleration (a_i) reaches a certain value, it overcomes the adhesion force of the dust deposited on the collecting electrode plates. The dust elements have a positive charge, and the collecting electrode plate has a negative charge [3,6,7]. As a result, the attraction force between them holds the dust in place. When the acceleration (a_i) overcomes this adhesion force, the deposited dust is separated from the surface of the collecting electrode plates and the surface of the discharge electrode rods.

Method of mechanical reflection [1, 3, 4]:

This section explains the method of mechanical reflection, which is a mechanical technique employed to estimate the strength of shear waves on a free surface, as well as to study the wave's shape and speed of wave propagation. The principle behind the mechanical reflection method is that when a force is applied to a suspension rod with a mass (m1), the shear wave propagates in the body to the free surface. If a ball (mass m2) is placed in contact with the free surface, under the influence of the shear wave, the ball bounces. Based on the displacement of the ball, the intensity of the shear wave on the free surface can be inferred (as shown in Figure 4).

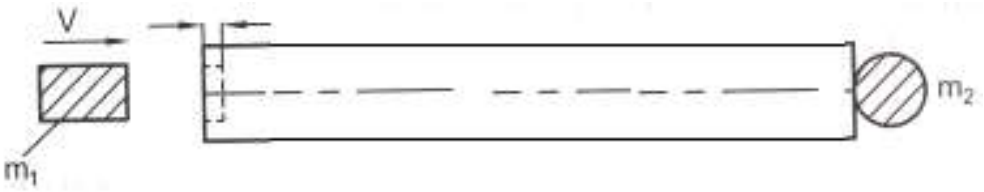

Figure 4. Deformation measurement diagram by mechanical reflection method

To measure the dust removal acceleration (a_i) in the collecting electrode plate, an experimental process is conducted according to the steps outlined in Figure 5. The sequence diagram illustrates the steps involved in the accelerometer experiment, which is a critical component of the experimental procedure for measuring stress wave acceleration in the collecting plate.

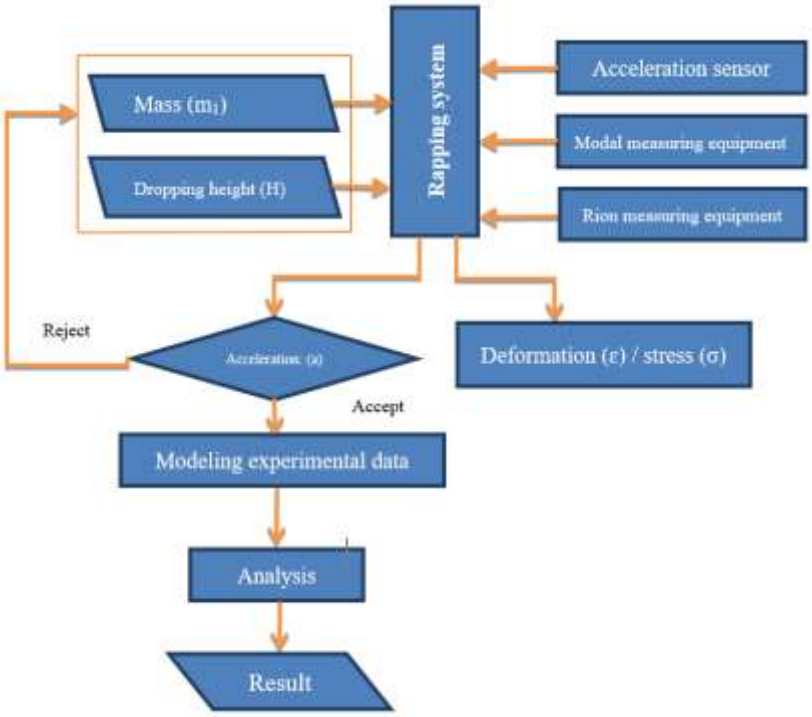

Figure 5. Sequence diagram of the accelerometer experiment

The mechanical reflection method is a valuable tool for studying shear waves in a variety of materials, including thin metal plates like the collecting electrode plate in this study. The method is highly accurate and provides valuable data on the strength and propagation characteristics of shear waves in various materials. By using this method in conjunction with other techniques, researchers can gain a more comprehensive understanding of the physical properties and behavior of materials subjected to various forms of stress and strain.

Experimental materials and models In this section, we will discuss the experimental materials and models used in the study. To ensure the accuracy and reliability of the results, the experimental model was designed to be uniform to the actual filter chamber in terms of size, structure, operating principle, kinetics, and dynamics. The structural image of the collecting electrode rapping set experimental model at the workshop of the National Research Institute of Mechanical Engineering (NARIME) is shown in Figure 6 [2].

Figure 6. Structural image of the collecting electrode rapping

Moreover, the hammer models used in the experiment were designed and fabricated based on an available design, and then assembled together by the riveting method. The structure of the hammer after assembling is shown in Figure 7. The hammer arm's structure (r) and the radius of rotation of the hammer (R) remained unchanged, and the mass of the hammer was varied based on the diameter dimension (D) with three different sizes.

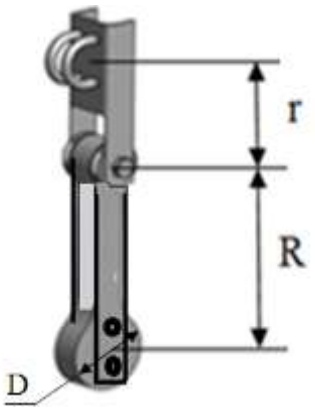

Figure 7. Structural model of hammer assembly

The experimental model used in the study was designed to be uniform to the actual filter chamber, and the materials used in the experiment were carefully selected to ensure accuracy and reliability. The hammer models used in the experiment were designed and fabricated based on an available design, and the structure of the hammer arm and the radius of rotation of the hammer remained unchanged, while the mass of the hammer was varied based on the diameter dimension with three different sizes.

Performing the experiment

The accurate execution of the experiment is essential to ensure that reliable data are obtained. The following steps are recommended to perform the experiment.

Step 1: Check the Atmosphere Conditions Before Performing the Experiment

Before starting the experiment, it is necessary to check the weather conditions. The accelerometer test should be carried out in dry weather conditions, at a temperature of approximately 25°C, and light wind level 2.

Step 2: Check the Technical and Technological Conditions of the Dust Rapping Model

To ensure that the experimental model is in optimal working condition, several technical and technological conditions must be checked, including:

Checking the position of the support hanger of the electrode sets to ensure there is no rusting. Suspension beams must be lubricated with dry grease to maintain one degree of freedom during the experiment.

Conducting a technical inspection of fixed bolt joints hanging the collecting electrode plates to the frame.

Ensuring that the collecting electrode plates are hooked together to form a secured block.

Verifying that the impact point between the hammer and the anvil is at the center point of the anvil.

Cleaning the surface of the collecting electrode plates thoroughly before attaching the measuring sensor.

Step 3: Check the Working Condition of Measuring Devices

It is essential to verify that all measuring devices are in working order and properly calibrated before starting the experiment. The following checks are recommended:

Checking the connection between the measuring device and the laptop, including the computer-connected measuring device and hand-held accelerometer.

Rechecking the calibration of measuring equipment to ensure accuracy.

Testing and checking the accelerometer signal.

Step 4: Establish the Accelerometer Measuring Grid

An accelerometer measuring grid must be established to ensure accurate and reliable measurements. This grid will help identify and locate any areas where the dust removal acceleration is weaker or stronger.

Step 5: Measure the Acceleration According to the Established Measuring Grid and Record the Measurement Results in the Summary Table

To measure the acceleration, follow these steps:

Attach the measuring sensor to the pre-defined position according to the measurement diagram.

Turn on measurement mode and sampling time on the measuring device.
Raise the hammer to the free fall position and let it collide with the anvil.
Read the measurement results.
Repeat the measurement three times at each measurement location and record the measurement data in the summary table.
Step 6: Data Processing
After obtaining the measurement results, the data must be processed to obtain the average values, standard deviations, and other statistical parameters. The data analysis can help identify any irregularities or discrepancies in the experimental results.

Experiment to determinate the dust removal acceleration and suitable impact force F of the hammer
Experimental process [1,2,5,7]

This section describes the experimental process used to measure the dust removal acceleration in the collecting electrode plates. The experiment was conducted under specific environmental conditions, including dry weather, a temperature of approximately 25°C, and light wind level 2, with the same technical and time conditions. The dust removal acceleration was measured by attaching the sensor to the defined position as described in the measuring grid, taking measurement data three times for each measuring location and recording the results in tables 1, 2, and 3. The hammer weight varied from 6 kg, 7 kg, and 8 kg, respectively. The objective of the experiment was to find a set of technological parameters of the dust collecting set that could create a dust removal acceleration range capable of separating deposited dust in conditions that ensured the durability of the collecting electrode plate. This would establish a variety of rapping hammer parameters, creating reasonable values of rapping force F that would satisfy the fatigue strength of the collecting electrode plate as well as the discharge electrode frame. From the experimental results of measuring the dust removal acceleration with the hammer mass varying from 6 kg, 7 kg, and 8 kg in table 1, it is observed that the measured dust removal acceleration values are within the acceleration limit range ($50g \leq a^* \leq 200g$) of the dry ESP equipment mentioned in the published documents [7]. The acceleration value at a measurement location according to the measuring grid was recorded as the average result of three different measurements under the same conditions and at the same time. These acceleration values were the basis for determining the stress wave propagation rule in the collecting electrode plates. Furthermore, in each accelerometer experiment, the average acceleration value over the total surface of the collecting electrode plate was also determined, thereby building a correlation relationship between rapping force and dust removal acceleration. Experimental measurement results are shown in tables 1, 2, and 3 corresponding to three types of hammer weight: 6 kg, 7 kg, and 8 kg. Table 1 shows the result of measuring acceleration relative to a hammer mass of 6 kg. The same measurement method was repeated for the other cases, with similar results for the 7-kg-mass hammer, where the average acceleration value was 1644 m/s^2, and for the 8-kg-mass hammer, where the average acceleration was 1790 m/s^2. These results provided important insights into the technological parameters required to achieve the desired dust removal acceleration range and rapping force values for the collecting electrode plates, ensuring their longevity and effectiveness.

Table 1. Result of measuring acceleration relative to hammer mass 6 kg

No.	Measurement point (a_{ij})	Experiment 1					
		Hammer weight (kg)	Rapping force F (Ns)	Dust removal acceleration a (m/s^2)			
				1st mea.	2nd mea.	3rd mea.	Ave.
1	a11	**6**	185.94	2217	2445	2259	**2307**
2	a12			1869	2062	1904	**1945**
3	a13			1860	2051	1894	**1935**
4	a14			1677	1708	1850	**1745**
5	a15			1724	1756	1902	**1794**
6	a16			1534	1562	1692	**1596**
7	a17			1479	1507	1631	**1539**
8	a18			1191	1213	1313	**1239**
9	a19			1090	1110	1202	**1134**
10	a21			1940	1977	2140	**2019**
11	a22			1827	1861	2015	**1901**

12	a23			1732	1764	1910	**1802**
13	a24			1622	1789	1653	**1688**
14	a25			1677	1850	1708	**1745**
15	a26			1420	1567	1447	**1478**
16	a27			1418	1565	1445	**1476**
17	a28			1100	1214	1121	**1145**
18	a29			980	1081	999	**1020**
19	a31			1858	2049	1892	**1933**
20	a32			1794	1979	1828	**1867**
21	a33			1759	1940	1792	**1830**
22	a34			1638	1806	1668	**1704**
23	a35			1627	1795	1657	**1693**
24	a36			1335	1472	1360	**1389**
25	a37			1336	1473	1361	**1390**
26	a38			994	1096	1012	**1034**
27	a39			920	1014	937	**957**
28	a41			1816	2003	1850	**1890**
29	a42			1713	1890	1746	**1783**
30	a43			1690	1865	1722	**1759**
31	a44			1738	1918	1771	**1809**
32	a45			1671	1515	1543	**1576**
33	a46			1548	1403	1429	**1460**
34	a47			1426	1293	1317	**1345**
35	a48			1046	949	966	**987**
36	a49			883	801	816	**833**
37	a51			1805	1637	1667	**1703**
38	a52			1823	1653	1684	**1720**
39	a53			1696	1538	1566	**1600**
40	a54			1896	1719	1751	**1789**
41	a55			1494	1354	1379	**1409**
42	a56			1483	1344	1370	**1399**
43	a57			1275	1156	1178	**1203**
44	a58			1160	1051	1071	**1094**
45	a59			730	806	744	**760**
Average value							**1543**

Setting up the experimental matrix to measuring acceleration:

In order to further analyze and interpret the measurement results of dust removal acceleration, an experimental matrix is established. The matrix is based on the measurement data obtained from tables 2 to 4. The matrix is shown in tables and is constructed using the following rules: The measuring points in the Y direction are denoted by i = 1 to 5, while the measuring points in the X direction are denoted by j = 1 to 9. The measurement results for each measuring point are recorded in matrix form according to the rules presented in tables 2, 3, and 4 for each hammer weight. The matrix format allows for a more organized and structured representation of the measurement results, which makes it easier to analyze and draw conclusions. By using this matrix format, the researchers can quickly identify the measurement results for each measuring point and hammer weight, and compare the data to determine if there are any significant differences. The establishment of this experimental matrix serves as a valuable tool for the analysis and interpretation of the measurement results, and helps to provide a more comprehensive understanding of the dust removal acceleration and suitable impact force of the hammer.

Table 2. Matrix of acceleration measurement results with hammer mass 6 (kg)

Vertical coordinate Y(m)	Horizontal coordinate for acceleration measurement X (m)									Ave. acc. (m/s^2)
	a_{ij}	0.32	0.96	1.6	2.24	2.88	3.52	4.16	4.7	5.34	
		a_{i1}	a_{i2}	a_{i3}	a_{i4}	a_{i5}	a_{i6}	a_{i7}	a_{i8}	a_{i9}	
14.5	a_{5j}	1703	1720	1600	1789	1409	1399	1203	1094	760	1543
11	a_{4j}	1890	1783	1759	1809	1576	1460	1345	987	833	
7.5	a_{3j}	1933	1867	1830	1704	1693	1389	1390	1034	957	
4	a_{2j}	2019	1901	1802	1688	1745	1478	1476	1145	1020	
0.5	a_{1j}	2307	1945	1935	1745	1794	1596	1539	1239	1134	

Table 3. Matrix of acceleration measurement results with hammer mass 7 (kg)

Vertical coordinate Y(m)	Horizontal coordinate for acceleration measurement X (m)									Ave. acc. (m/s^2)
	a_{ij}	0.32	0.96	1.6	2.24	2.88	3.52	4.16	4.7	5.34	
		a_{i1}	a_{i2}	a_{i3}	a_{i4}	a_{i5}	a_{i6}	a_{i7}	a_{i8}	a_{i9}	
14.5	a_{5j}	1900	1798	1689	1567	1580	1432	1089	998	858	1644
11	a_{4j}	1980	1802	1862	1655	1789	1577	1232	1085	940	
7.5	a_{3j}	1954	1879	1896	1865	1665	1700	1345	1343	1132	
4	a_{2j}	2100	2008	1978	1768	1656	1726	1487	1477	1243	
0.5	a_{1j}	2213	2109	2003	1956	1889	1790	1677	1588	1389	

Table 4. Matrix of acceleration measurement results with hammer mass 8 (kg)

Vertical coordinate Y(m)	Horizontal coordinate for acceleration measurement X (m)									Ave. acc. (m/s^2)
	a_{ij}	0.32	0.96	1.6	2.24	2.88	3.52	4.16	4.7	5.34	
		a_{i1}	a_{i2}	a_{i3}	a_{i4}	a_{i5}	a_{i6}	a_{i7}	a_{i8}	a_{i9}	
14.5	a_{5j}	1998	1867	1720	1789	1730	1682	1420	1329	1206	1790
11	a_{4j}	2008	1980	1857	1854	1893	1789	1567	1403	1330	
7.5	a_{3j}	2100	1912	1901	1933	1832	1865	1670	1589	1458	
4	a_{2j}	2301	2102	1983	2011	1902	1930	1743	1674	1324	
0.5	a_{1j}	2333	2213	2207	2128	2004	1978	1730	1712	1632	

Empirical regression function graph of acceleration distribution in the collecting electrode plate:

When a force is applied to the collecting plate by the hammer, dust removal acceleration propagates on the surface of the plate. The stress wave propagation in the plate decreases in the direction away from the impact area and remains stable before the rapping force ends. To choose a regression function representing the distribution of the dust removal acceleration in the collecting electrode plate, it is necessary to check the distribution of the dust removal acceleration in the electrode plate at different measuring heights through the measured acceleration values. If the rule of argument values changes exponentially (addition/multiplication), based on that, the corresponding regression function will be selected [4].

Table 5 Ratio of argument values of experimental results

No.	Results								
	Plate 1	Plate 2	Plate 3	Plate 4	Plate 5	Plate 6	Plate 7	Plate 8	Plate 9
K_5/K_4	1.109806	1.036628	1.099375	1.011179	1.118523	1.043602	1.118038	0.902193	1.096052
K_4/K_3	1.022751	1.047112	1.040364	0.941957	1.074238	0.951369	1.033457	1.047619	1.148859
K_3/K_2	1.04449	1.018211	0.984699	0.99061	1.030714	1.064074	1.061870	1.107350	1.065830
K_2/K_1	1.142645	1.023146	1.073807	1.033768	1.052199	1.079837	1.042682	1.082096	1.111764

In this regard, the coefficients ($K_{i+1}/K_i = Y_i+1/Y_i$) of columns X_{i1} to X_{i4} were checked, and the results are shown in Table 5. From Table 5, it is observed that the values of the coefficient K are almost unchanged and asymptotic to the value 1. Therefore, based on the experiment planning documents [2], it is possible to represent the dust removal acceleration distribution in the collecting electrode plate using the following power function:

$$Y = b_0 . e^{b1 . X} \quad (20)$$

To obtain the experimental graphs, the data analysis statistics method SPSS was applied, and the graph type was chosen as the regression type. The regression equations for three types of experiments were displayed, and the experimental graphs were created, as shown in figures a), b), c) of Figure 8. From the data processing results, the regression graph of the distribution of dust removal acceleration on the collecting electrode plate measured in three regions on the surface of the plate was obtained (Figure 8).

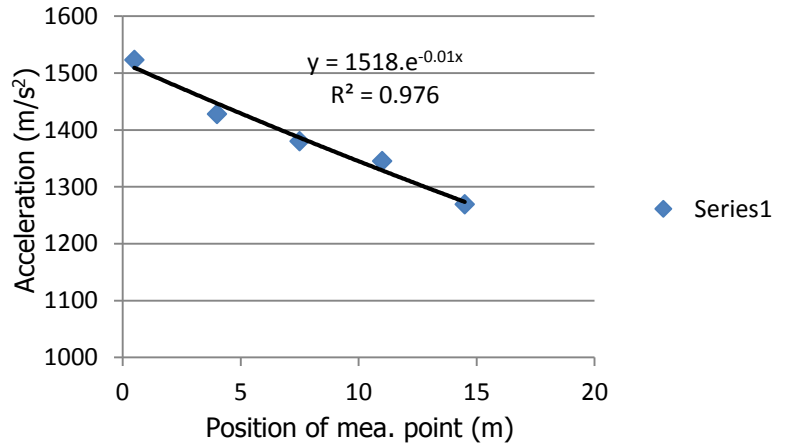

a) Experiment No. 1

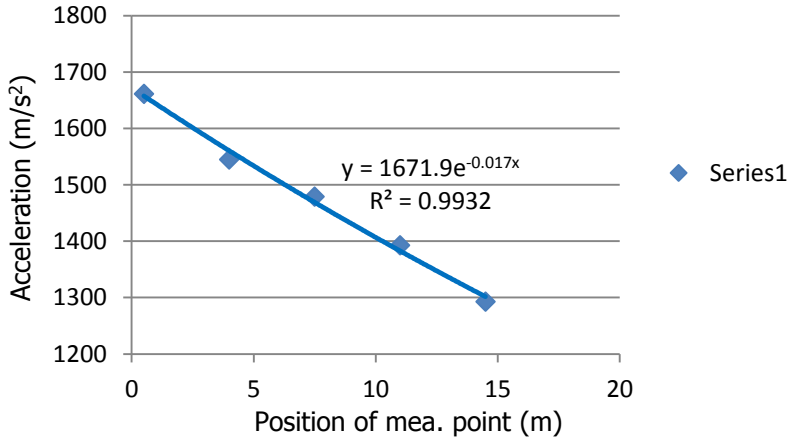

b) Experiment No. 2

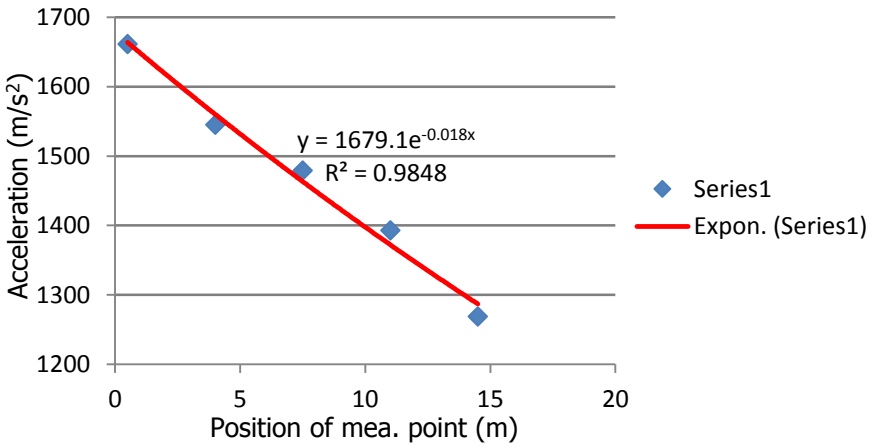

c) Experiment No. 3

Figure 8. Experimental graph of dust removal acceleration distribution in collecting electrode plate

To create a graph according to the magnitude of the dust removal acceleration value in the collecting electrode plate, the experimental data in Table 1 was used. Figure 9 shows the experimental graph of the dust removal acceleration distribution in the collecting electrode plate corresponding to the hammer weight (6 kg, 7 kg, 8 kg) a), b), c), respectively.

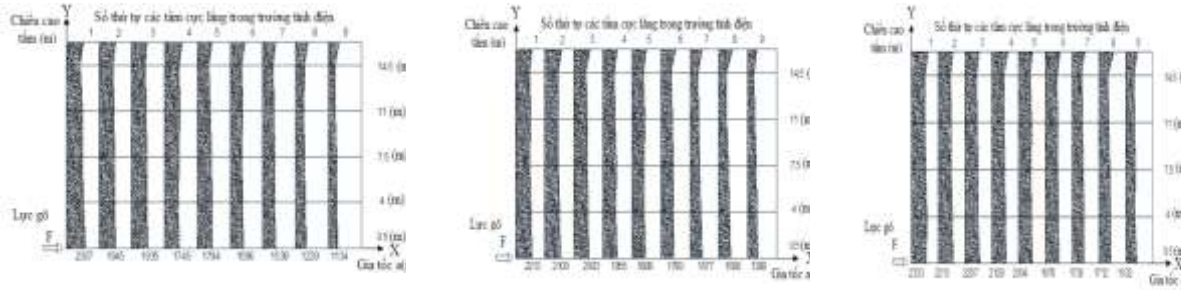

Figure 9. Experimental graph of dust removal acceleration distribution in the collecting electrode plate a), b), c) corresponding to the hammer weight (6 kg; 7 kg; 8 kg)

Determination of dust removal rapping force, ensuring the durability of the main parts of the dust filtering chamber [6]

In order to ensure the durability of the main parts of the dust filtering chamber, it is necessary to determine the dust removal rapping force. This force is calculated using the formula (21) given below:

$$F = 0.032 + 0.0785H + 16.080m_1 + 30.42m_1H \quad (21)$$

The formula (21) takes into account the impact force of the hammer and the durability limit of the collecting electrode plate material. The regression equation (21) shows the influence weight and the interaction between variables such as hammer mass (m_1) and falling height (H) to the rapping force value (F).

The yield strength of the test materials should be similar to CT3 steel, which was a former Soviet standard. For materials with a yield strength of σ_{ch} = 250 Mpa = 25 (kN/cm²), it is necessary to choose a factor of safety k = 0.8 to ensure that the equipment operates within the yield strength of the material. The allowable yield strength $[\sigma_{ch}]$ can then be calculated as:

$$[\sigma_{ch}] = k*\sigma_{ch} = 0.8*25 = 20 \text{ (kN/cm}^2\text{)} \quad (23)$$

It is important to ensure that the rapping force value does not exceed the allowable yield strength of the material. This will help to ensure that the equipment operates safely and within its expected lifespan.

Scientific discussion about the achieved results

The experimental results provide insights into the behavior of dust removal acceleration in the collecting electrode plate under the impact of the hammer. Figures 8 and 9 illustrate that the acceleration value in the collecting electrode plate is highest within the area of impact of the hammer, and then gradually stabilizes to a constant value. It can be observed that the propagation of the stress wave in the plate decreases in the direction away from the impact area and remains at a stable value

before the rapping force ends. Moreover, the results show that the distribution of the dust removal acceleration in the collecting electrode plate is nonlinear. Hence, it is necessary to use a non-selective function to represent the rule of acceleration values distribution on the collecting electrode plate. The obtained regression function in equation (21) represents the distribution of the dust removal acceleration in the collecting electrode plate in terms of power function. The achieved results provide crucial insights into the selection of the hammer mass (m_i) and the corresponding rapping force values (F) that meet the fatigue strength of the collecting plate. The regression equation (21) shows that the rapping force value (F) is dependent on the hammer mass (m_1) and falling height (H) and their interaction. The experimental results discussed in this section demonstrate the importance of choosing an appropriate hammer mass and falling height to achieve effective dust removal without compromising the durability of the main parts of the dust filtering chamber. Moreover, the nonlinearity of the dust removal acceleration distribution in the collecting electrode plate highlights the significance of selecting an appropriate function to represent the distribution rule.

3. Conclusion

The experimental results presented in this study have led to the following conclusions:

1) This study has contributed to the advancement of knowledge in Vietnam by applying the theory of stress wave propagation in thin metal sheets to explain the impact of rapping force (F) and the stress wave propagation process that creates dust removal acceleration (a) for the collecting electrode plate. This is the first time that such a theory has been applied in Vietnam.

2) The study has established an experimental model and selected modern measuring equipment, such as Modal analysis and Rion VA-12, to measure the dust removal acceleration (a) in the collecting electrode plate. The study also determined the test limit conditions of propagating wave acceleration {$50g \leq a \leq 200g$ (m/s^2) and strength limit of electrode plate materials $[\sigma_{ch}] \leq 18$ (kN/mm^2) [4]; hammer weight limit: 6 (kg) – 8 (kg); ratio factor between the mass of the hammer and electrode set: $K = m_1/m_2 = 0.0066 \div 0.0088$; drop height limit of the hammer: $0.49m \leq H \leq 0.57$ (m) [2] as the basis for determining the optimal technological parameter domain of rapping hammer.

3) The study established an empirical regression equation between the hammer mass (mi), hammer drop height (hi) with rapping force (F) and the function describing the relationship between the rapping force (F) and the dust removal acceleration (a). The regression equation is as follows:

$$\begin{cases} F = 0.032 + 0.0785h + 16.080mi + 30.42mi\,h \leq F^* \\ a = 794.5 + 3{,}99\,F \leq a^* \end{cases}$$

4) The results of this study have opened up the possibility of localizing the calculation and design of the filter chamber, which is the main component of many horizontal electrostatic precipitators with variable capacities widely used in Vietnam. In summary, this study has contributed significantly to the advancement of knowledge in the field of dust removal in electrostatic precipitators in Vietnam. The results can be used to improve the design and operation of such systems, ultimately leading to better air quality and a safer environment.

4. References

Nguyen Van Vuong (2008). Stress wave propagation in objects. Bach Khoa Publishing House.

Nguyen Tien Sy (2020). "Research on the impacts of specification varieties of the rapping hammer system for the collecting electrodes of the ESP related to dust removal ability."

Манжов В.К. Longitudinal impact models. Ulyanovsk, 2006.

Писаренко Г.С. Handbook of strength of materials, НАУКОВА ДУМКА, 1976.

Schwarz, B. J., & Richardson, M. H. (1999). Experimental modal analysis. CSI Reliability Week, Orlando.

Allemang, R. J. (1998). Vibration, analytical and experimental modal analysis. University of Cincinnati, Ohio.

Дейвис Р.М. Stress waves in solids. Translation from English edited by G. S. Shapiro. Moscow, Foreign Literature Publishing House, 1981.